



## Article

# The Influence of Visual Landscapes on Road Traffic Safety: An Assessment Using Remote Sensing and Deep Learning

Lili Liu <sup>1</sup> , Zhan Gao <sup>1</sup>, Pingping Luo <sup>2,3,4,\*</sup> , Weili Duan <sup>5</sup>, Maochuan Hu <sup>6</sup> ,  
Mohd Remy Rozainy Mohd Arif Zainol <sup>7</sup> and Mohd Hafiz Zawawi <sup>8</sup>

<sup>1</sup> Chang'an University, Xi'an 710061, China; lilyliu@chd.edu.cn (L.L.); gaozhan@chd.edu.cn (Z.G.)

<sup>2</sup> School of Water and Environment, Chang'an University, Xi'an 710054, China

<sup>3</sup> Key Laboratory of Subsurface Hydrology and Ecological Effects in Arid Region, Ministry of Education, Chang'an University, Xi'an 710054, China

<sup>4</sup> Xi'an Monitoring, Modelling and Early Warning of Watershed Spatial Hydrology International Science and Technology Cooperation Base, Chang'an University, Xi'an 710054, China

<sup>5</sup> State Key Laboratory of Desert & Oasis Ecology, Xinjiang Institute of Ecology & Geography, Chinese Academy of Sciences, Urumqi 830011, China; duanweili@msxjb.ac.cn

<sup>6</sup> School of Civil Engineering, Sun Yat-sen University, Guangzhou 510275, China; humch3@mail.sysu.edu.cn

<sup>7</sup> River Engineering and Urban Drainage Research Centre (REDAC), Universiti Sains Malaysia, Nibong Tebal 14300, Malaysia; cereum@usm.my

<sup>8</sup> Department of Civil Engineering, Universiti Tenaga Nasional (UNITEN), Kajang 43000, Malaysia; mhafiz@uniten.edu.my

\* Correspondence: lpp@chd.edu.cn; Tel.: +86-29-82339376

**Abstract:** Rapid global economic development, population growth, and increased motorization have resulted in significant issues in urban traffic safety. This study explores the intrinsic connections between road environments and driving safety by integrating multiple visual landscape elements. High-resolution remote sensing and street-view images were used as primary data sources to obtain the visual landscape features of an urban expressway. Deep learning semantic segmentation was employed to calculate visual landscape features, and a trend surface fitting model of road landscape features and driver fatigue was established based on experimental data from 30 drivers who completed driving tasks in random order. There were significant spatial variations in the visual landscape of the expressway from the city center to the urban periphery. Heart rate values fluctuated within a range of 0.2% with every 10% change in driving speed and landscape complexity. Specifically, as landscape complexity changed between 5.28 and 8.30, the heart rate fluctuated between 91 and 96. This suggests that a higher degree of landscape richness effectively mitigates increases in driver fatigue and exerts a positive impact on traffic safety. This study provides a reference for quantitative assessment research that combines urban road landscape features and traffic safety using multiple data sources. It may guide the implementation of traffic safety measures during road planning and construction.

**Keywords:** deep learning; semantic segmentation; traffic safety; driving performance; remote sensing; street view image; visual landscape elements



**Citation:** Liu, L.; Gao, Z.; Luo, P.; Duan, W.; Hu, M.; Mohd Arif Zainol, M.R.R.; Zawawi, M.H. The Influence of Visual Landscapes on Road Traffic Safety: An Assessment Using Remote Sensing and Deep Learning. *Remote Sens.* **2023**, *15*, 4437. <https://doi.org/10.3390/rs15184437>

Academic Editor: Francesco Nex

Received: 9 July 2023

Revised: 22 August 2023

Accepted: 4 September 2023

Published: 9 September 2023



**Copyright:** © 2023 by the authors. Licensee MDPI, Basel, Switzerland. This article is an open access article distributed under the terms and conditions of the Creative Commons Attribution (CC BY) license (<https://creativecommons.org/licenses/by/4.0/>).

## 1. Introduction

With the rapid growth of the global population and economy, urban road networks continue to expand, and the number of vehicles on the road is steadily increasing each year. As a consequence, traffic accidents are becoming more frequent. According to a report by the World Health Organization (WHO) in 2018, over 1.3 million people die in road traffic accidents every year. This leads to significant loss of life, property damage, and adverse environmental impacts, all of which are detrimental to the sustainable development [1,2]. During the process of driving on roads, the increasing frequency of traffic accidents caused by visual landscapes [3,4] necessitates the exploration of a new approach to integrate a

large amount of data to represent the visual environment of drivers on the road and to investigate its impact on driving safety [5].

In previous studies examining the influence of visual landscapes on traffic safety, researchers have primarily focused on how drivers perceive visual environments on roads [6] by contrasting people's reactions to natural elements versus artificial elements and uniform environments versus diverse environments during road usage [7,8], researchers have gained insights into the preferences of car users for road environments [9]. In recent years, research on the effects of road environments on driver behavior and safety has become a focus. Studies using driving simulators have investigated the impact of road environments on driving speed and reaction time, demonstrating that the environment is an essential factor that influences driver workload and performance [10]. Based on a survey, researchers revealed the significant influence of driving environments on speeding and overtaking violations [11]. Poor highway landscapes can lead to adverse driving performance, dangerous driving behavior, and traffic accidents [12]. Conversely, a well-designed road landscape can positively impact the physical and mental states of drivers, thereby promoting traffic safety and reducing accident occurrences [13]. Research examining the influence of trees on collision frequency in urban areas has shown that a higher tree density can reduce traffic accidents [14]. In a study conducted on the Qinghai-Tibet Highway, researchers used plant landscape color values and driver blink frequency as analysis indicators, reflecting how a pleasant road landscape environment can provide drivers with a comfortable visual experience.

In recent years, extracting road information from remote sensing images has become the primary method for updating road information, ensuring both accuracy and automation [15,16]. High-quality road information updates are important for intelligent urban planning, sustainable urban development, vehicle management, and traffic navigation [17,18]. These algorithms require a high resolution, road curvature, and boundary conditions [19–21]. With the availability of increasingly rich street-view map resources [22], which provide new perspectives and research methods, researchers can supplement the details of urban perception from a human perspective [23]. Street-view images, such as those with temporal and spatial information, comprehensively display road landscapes and provide a sense of immersion [24]. Consequently, more studies have begun utilizing street-view images to visually represent landscape features and explore people's visual perception of open environments [25,26]. Companies like Google and Baidu have used street-view images for road detection, classification, and mapping [27,28]. The digital resources of urban road networks are crucial for industrial applications and are key requirements for digital cities to reduce road traffic accidents [29]. The rapid development of computer vision applications has provided powerful feature extraction capabilities, enhancing the understanding of semantic information contained in street-view images and significantly improving the ability to perceive urban scenes [30], thereby providing a new quantitative means for obtaining road landscape features.

In the field of driving safety research, deep learning algorithms were first employed to calculate traffic volume and detect traffic speeds [31]. Subsequently, they have rapidly advanced in areas such as vehicle kinematics, vehicle behavior tracking, and place information extraction. Some studies have utilized detection and tracking algorithms to obtain vehicle trajectories and calculate surrogate safety measures [32,33]. Others have provided obstacle avoidance solutions by observing the collision rates of vehicles in intersection environments [34]. Tanprasert et al. developed an algorithm for extracting information regarding objects surrounding roads from street-view images based on distance perception accumulation, thereby enabling the assessment of traffic environment safety [35]. Mooney et al. found a significant correlation between environmental infrastructure and the number of accidents and evaluated the impact of the environment on crash frequency [36]. Li et al. developed an algorithm to depict the visual glare situation for drivers and estimate the time window of sun glare by calculating the sun's position and the relative angle between the driver and the sun at different locations [37]. These studies achieved high-precision

results and involved extensive video and image collection. However, many important factors related to the driver's field of view have not been extracted from videos and images, and their impact on safety has not been explored. Therefore, there is an opportunity to further explore the application of deep learning to driving safety.

This study employs a method that integrates street view imagery with deep learning to propose an effective framework for extracting road visual elements, capturing both clustering and depth information from images [38]. To further enrich our data sources, we have utilized the latest 2023 version of remote sensing data from geographic data repositories, such as OpenStreetMap. This is done to complement the structural features of road networks and capture other essential details. These details encompass elements such as green spaces, urban features, architectural diversity, and more, enabling us to comprehensively examine a variety of landscapes and visual elements within the driving environment from multiple perspectives [39]. The outcomes of this study can offer valuable insights for formulating detailed measurement indicators pertaining to urban road environment characteristics. Moreover, this research takes a holistic approach by considering environmental features and the driver's physical condition, resulting in the construction of a quantitative relationship model to explore the correlation between driving speed, landscape complexity, and driver heart rate. This model is utilized to evaluate the extent to which the visual environment impacts road safety. We hope that the outcomes of this study will introduce novel insights for enhancing road traffic safety by addressing road visual landscapes. Furthermore, the study aims to provide theoretical support for enhancing road landscape planning, thus contributing to the achievement of sustainable development objectives.

In the following section, this study presents the research area and the data collection process used in the study. Section 3 discusses the distribution characteristics of urban road landscape elements, presents the model-fitting results, and conducts an analysis of the findings. Section 4 summarizes the contributions of this research and proposes paths for further exploration using the conclusions obtained in this study. The final section discusses the novelty of the research outcomes and strategies for applying them in practical applications, combining the research findings with real-world practices.

## 2. Data and Methods

### 2.1. Study Area

As shown in Figure 1 (<https://search.asf.alaska.edu/#/>, accessed on 20 April 2023), Xi'an is the capital of the Shaanxi Province in China and has a temperate monsoon climate [40–42]. It is an important central city in Western China, a core city in the Guanzhong Plain urban agglomeration, and a demonstration city promoting new energy vehicles [43]. At the end of 2022, the population of Xi'an was 12.96 million people, with a total of 4.8588 million motor vehicles, representing the seventh-highest number of vehicles in the country. The Traffic Health Index refers to an indicator that measures the percentage of proximity to the optimal traffic conditions. It has consistently remained at around 40%, indicating a significant gap compared to the ideal state. The suboptimal traffic health issue in Xi'an City is becoming increasingly prominent. In addition, as a city with a history of being the ancient capital of thirteen dynasties, Xi'an attracts a large number of tourists with its abundant tourism resources. This influx of tourists has also significantly contributed to the substantial traffic volume in the city.

The Xi'an Ring Expressway forms a circular high-speed thoroughfare around the outskirts of the city, connecting the national trunk roads. For this study, we selected a section of the G3002 Ring Expressway within the Yanta District of Xi'an, from the Lihua Shui Interchange to the Chanhe East Road intersection, as the study area. The Yanta District is a nationally renowned area for science, education, culture, and tourism. The selected section of the expressway is 26 km long, with a roadbed width of 35 m. It is a fully enclosed, all-interchange, six-lane highway with a green area of 1.683 million m<sup>2</sup> on both sides of the road. The area passes through industrial clusters, integrates cultural tourism, encompasses

major historical sites, and emphasizes ecological functionality [44–46], providing a diverse environment. Traffic accidents on the Ring Expressway account for 0.5% of the total number of accidents in the Yanta District, indicating a relatively high accident rate. The road network also experiences prolonged delays owing to high traffic demand. With the growth of the city's population and economy, the imbalance between transportation supply and demand exerts significant pressure on traffic safety on the Ring Expressway.

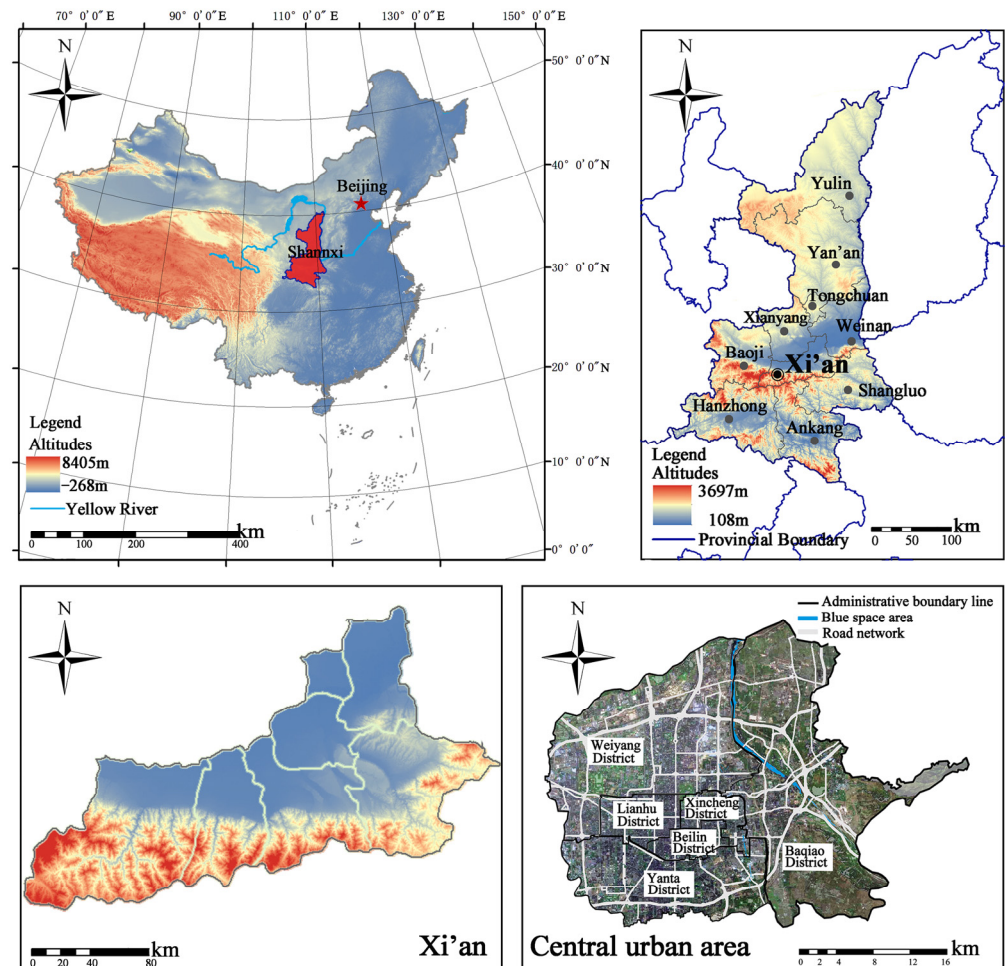


Figure 1. Study area.

## 2.2. Research Framework

The characteristics of the road environment are relevant to risk factors in driver fatigue development during driving. In order to extract urban road environment features and quantitatively analyze the impact of landscapes on driving behavior, this paper constructs the research framework as illustrated in Figure 2. Firstly, prior road knowledge, such as OSM data (Open Street Map) [47], is utilized to extract road morphology, assisting in generating street view sampling points while excluding construction and closed roads, thereby obtaining clear road lines in street view. Subsequently, street view collection points are uniformly segmented every 50 m along the road lines to acquire street view images. A convolutional neural network algorithm is then employed to segment the images, extracting features of visual landscape elements in road street view images, including the green-looking ratio, street openness, building view index, and landscape complexity, representing the driver's visual landscape characteristics [48]. These features are accurately displayed on the map (<http://guihuayun.com/maps/index.php>, accessed on 20 April 2023).

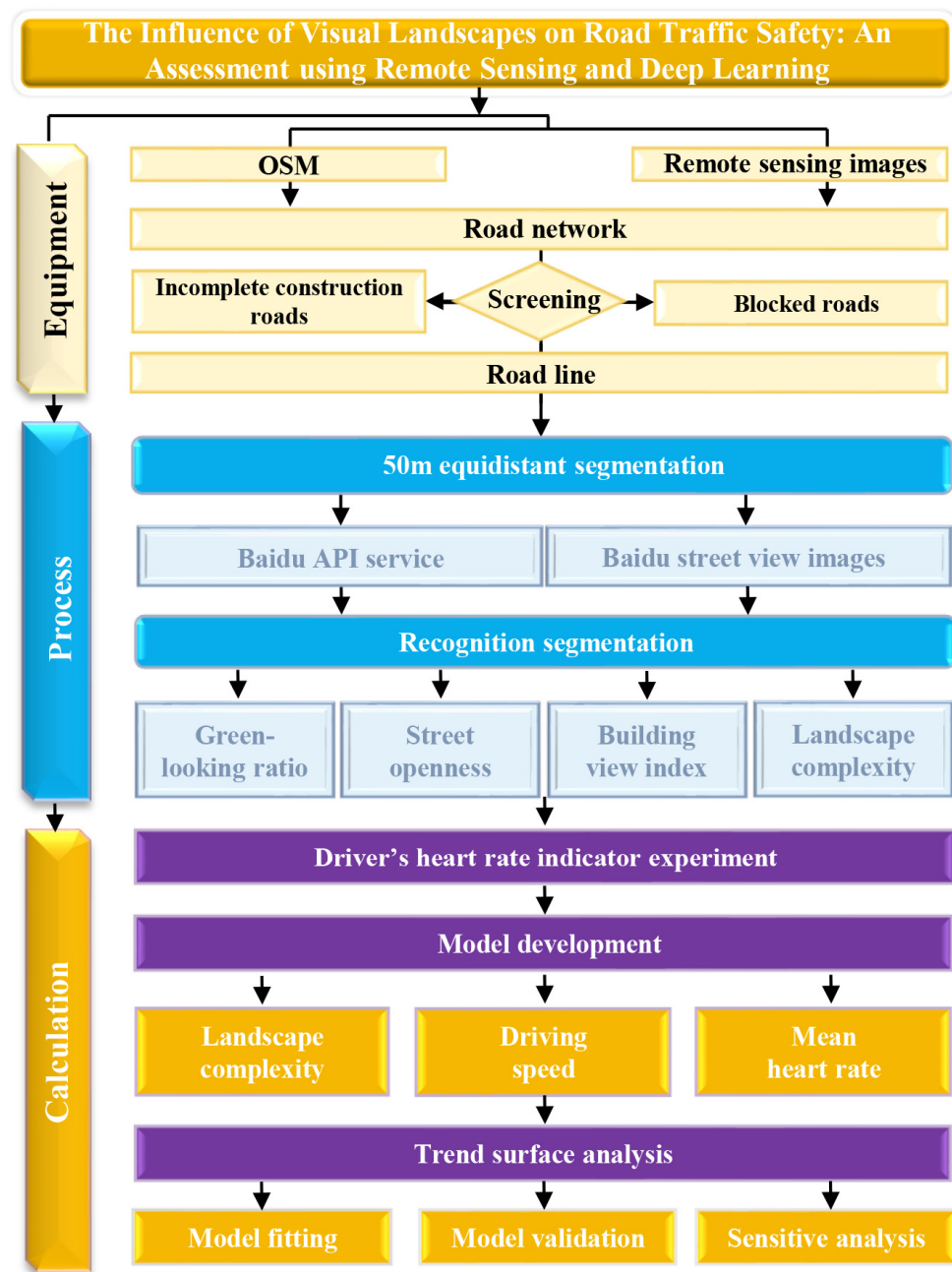


Figure 2. Research framework for the present study.

The mean heart rate (MHR) is closely associated with driver fatigue and is commonly used to identify driver fatigue status [49–51]. Therefore, the next step involved collecting physiological signals of driver heart rate in driving environments to investigate the combined effects of highway landscape and driving speed on driver heart rate. To establish a joint relationship model among the three factors, we chose landscape complexity and driving speed as independent variables, while driver heart rate was considered the dependent variable.

### 2.3. BSVI Data Collection

The application of street-view images to the analysis of urban road networks and environmental quality has become increasingly common in the field of urban science [52]. Street-view data provide unique opportunities for human-centered observations in urban environments [53,54].

To comprehensively assess the environmental features of the Xi'an Ring Expressway, we retrieved Baidu Street View Images based on locations from the Baidu Map Open Platform and sampling points. First, the street network coordinate system downloaded from OSM (<https://www.openstreetmap.org/>, accessed on 20 April 2023) was calibrated. We randomly generated 1002 street-view sampling points at 50-m intervals, with latitude and longitude coordinates as the basis for input parameters in the Baidu Street View Map Application Programming Interface (API). Subsequently, to ensure a correct and complete view in all directions from each street-view point, a Python program was used to access the Baidu Map API and collect the panoramic images (Figure 3).

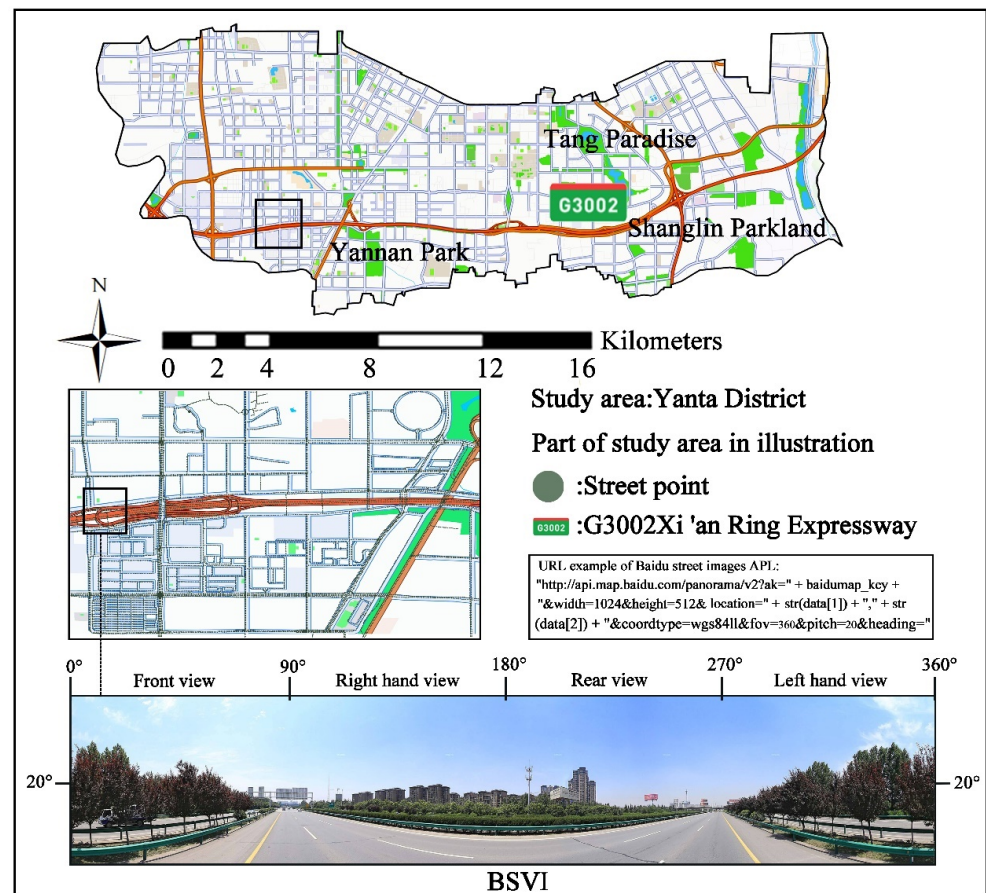


**Figure 3.** Example of a panoramic street-view image using Baidu Maps Application Programming Interface.

To accurately simulate the perception of driver driving, we used the following specific parameter settings to retrieve Baidu Street View Images (BSVIs) from the API. Geographical latitude and longitude coordinates were converted to the Baidu Street View Map standard BD09, the vertical angle (pitch) was set to  $0^\circ$ , the field of view was set to  $360^\circ$ , and the maximum pixel size was set to  $1024 \times 512$  to ensure high-quality access to images. To ensure the reliability of the analysis of the environmental characteristics of the Ring Expressway, invalid access results and blurry images were filtered out, and duplicate sampling points were cleaned. Finally, using Python and the Baidu Street View Map API, 990 street-view images were obtained based on the sampling points.

#### 2.4. Extraction of Drivers' Visual Environment Elements from BSVIs

To extract information from images and compute it, we applied deep learning techniques, particularly the image semantic segmentation [54]. As a key technology for the understanding of a visual scene, semantic image segmentation accurately identifies dif-

ferent objects in an image instance by assigning classification labels to each pixel. The scale of the training dataset primarily determines the number of object categories that the segmentation model can recognize [55]. Considering the remarkable performance of the deep learning fully convolutional network (FCN) image segmentation technique in urban exploration in China, we employed the publicly-available ADE-20K dataset, which was released by the Massachusetts Institute of Technology, for precise recognition and pixel-level classification, as well as semantic segmentation of elements in 150 everyday life scenes, including sky, road, car, and plants. Using this dataset, the fundamental visual environmental elements and environmental characteristics of the study area were obtained. Figure 4 shows the original BSVIs along with the corresponding results of visual element segmentation, identifying distinct objects in the images, and computing the coverage percentage of each visual element in the street-view images through cluster analysis. The color matrix at the bottom represents the semantic segmentation information of the extracted visual elements.

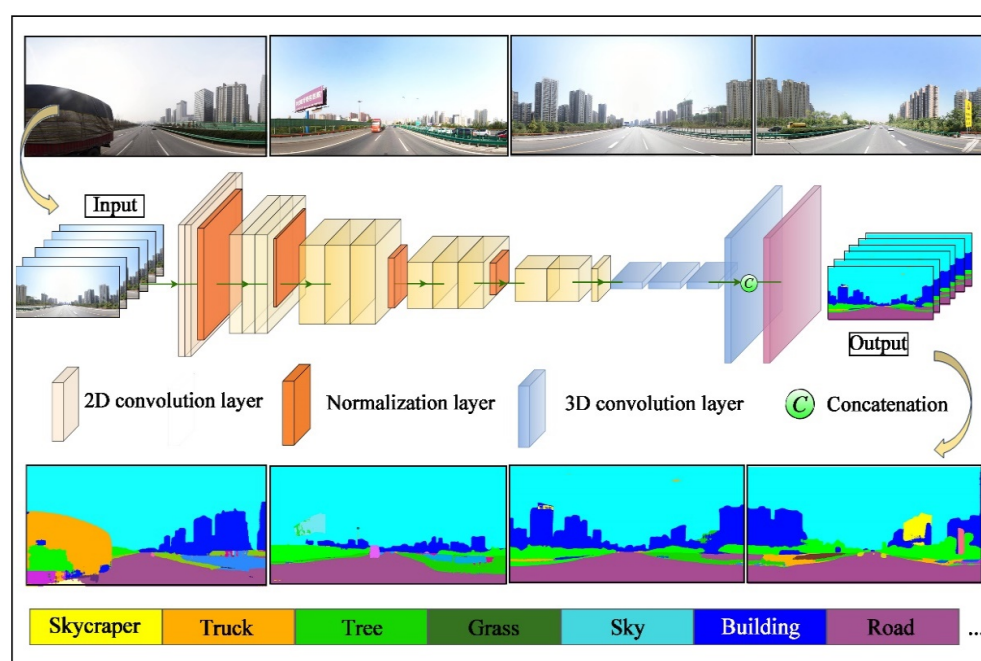


**Figure 4.** Extracting highway visual environment elements from street-view images using image semantic segmentation models.

The primary visual landscape elements of urban road environments are the green-looking ratio, street openness, building view index [56], and landscape complexity [57]. The level of greenery is meaningful for driving performance in terms of creating a sense of relaxation [58,59] and controlling driving speed [60]. In high-density urban environments, an adequate sky view plays a significant role in shaping the visual landscape experience [61]. The impact of the sky openness on urban traffic planning has become a prominent issue, particularly in the context of ongoing global warming and rapid urbanization. The built environment [62] affects driving safety through driver line-of-sight guidance [63] and perception of speed differences [64]. The landscape complexity of different driving environments influences traffic collisions by affecting driver decision-making, attention restoration [65], and traffic conflict [66]. Based on this, we extracted and analyzed the semantic segmentation results of street-view images to obtain basic information on the visual landscape elements of the Xi'an Ring Expressway (Table 1).

**Table 1.** Definitions and equations for four visual landscape elements.

Order Number	Feature Elements of Road Space	Concrete Content	Objective Score Equations (Based on Their Operational Definitions)
1	Proportion of road elements	$VI_{feature}$ denotes the view index of a physical feature (proportion of the visual element's pixels in a street view imagery),	$VI_{feature} = \frac{\sum_{i=1}^n PixeI_{feature}}{\sum_{i=1}^n PixeI_{total}} = \frac{1}{n} \sum_{i=1}^n PixeI_{feature},$ $feature \in (tree, building, sky, grass, etc)$ (1)
2	Green-looking ratio	The ratio of street visible greening to all pixel points in street view images.	$Greenx_i = VI_{tree} + VI_{grass} + VI_{plant}$ (2)
3	Street openness	The proportion of sky elements in the pixels of street view images.	$Skyx_i = VI_{sky}$ (3)
4	Building view index	The proportion of buildings, houses, skyscrapers in all pixel points in street view images.	$Bldgx_i = VI_{building} + VI_{house} + VI_{skyscraper} + VI_{tower}$ (4)
5	Complexity	The visual richness of a place, which depends on the variety of the numbers and types of buildings, ornamentation, landscape elements, street furniture, signage, and human activity	$Cmplx_i = \frac{Greenx_i + VI_{rail} + VI_{signboard} + VI_{pole} + VI_{car} + VI_{mountain}}{Bldgx_i + VI_{road}}$ (5)

## 2.5. Driver Heart Rate Indicator Experiment

### 2.5.1. Data Collection from Field Experiments

To advance this research, a model was developed to analyze the impact of visual landscape features on the driving states of drivers. We conducted a real road experiment on a specific section of the Xi'an Ring Road, namely the Lihuashui Interchange to the Chanhe East Road intersection in the Yanta District of Xi'an. During the experiment, we collected relevant heart rate data to assess driver fatigue levels. Our objective was to examine the influence of visual landscape complexity on driving safety and determine the parameters within the relationship model.

To obtain comprehensive and objective data, the experiment was conducted during daytime hours with a lower traffic volume to minimize the impact of non-road environmental factors on drivers. To ensure safety, we required the participating drivers in the driving experiment to be in good physical condition, maintain regular sleep patterns, possess a valid driver's license, have ample driving experience, and fall within the age range of 23 to 40 years, with no history of adverse driving records or involvement in serious accidents. Among the 30 participants, the ratio of male to female drivers was 1:1, with an average age of 31.2 years and an average driving experience of 4.7 years. On the day before the experiment, their sleep conditions were normal, and in the 12 h leading up to the trial, they abstained from consuming any medication, alcohol, coffee, or other stimulating beverages. Prior to the start of the experiment, the experimenter provided the participants with basic information about the purpose of the study, the experimental procedure, and any relevant instructions. Throughout the entire duration of the experiment, participants were not allowed to use their phones or other electronic devices, and the experimenter maintained a quiet environment. To ensure driving safety, the participants were given designated rest periods when they felt fatigued.

As shown in Figure 5, to ensure synchronous data acquisition and facilitate subsequent matching of visual environmental complexity with street views, a camera was placed inside the vehicle (below the windshield, in front of the passenger seat) to continuously record roadside landscapes. The design speed range of the Xi'an Ring Expressway is between 60 km per hour and 120 km per hour. As a crucial part of the urban expressway network, this road segment experiences relatively dense traffic flow and operates at a slower driving pace. To conduct safe experiments while the vehicle was in motion, upon entering the experimental section, the vehicle maintained an initial speed of 60 km per hour for 1 km. After confirming a stable heart rate, the speed was increased by 1 km per hour every 2 min. Data collection for the measured heart rate and vehicle speed was performed at 2-min intervals. Considering individual differences, multiple individuals simultaneously read and recorded data to obtain an average heart rate value to reduce measurement errors. Figure 5 illustrates the details of the experimental equipment and field experiments.



**Figure 5.** Real vehicle experimental devices. (a) Devices used in real vehicle experiments; (b) Debugging preparation.

### 2.5.2. Construction of a Relationship Model for the Effect of Highway Visual Landscape Complexity on Heart Rate Considering Driving Speed

Heart rate reflects the rhythmic activity of the human heart and is a relatively stable physiological signal that varies continuously over time. Under different external stimuli, the characteristics of heart rate values may vary, reflecting the impact of visual landscape features on an individual's level of excitement, fatigue, and concentration at different driving speeds.

To ensure the effectiveness of the analysis, the study collected 31 sets of data. The processed variables  $x$ ,  $y$  and  $z$  were subjected to regression analysis, resulting in  $z = f(x, y)$ . When the minimized residual sum of squares ( $Q$ ), where the squared difference between the actual values  $z_i$  and the predicted values  $f(x_i, y_i)$  is the smallest, indicates a trend surface fitting in the sense of the least squares method. Therefore, the trend surface analysis method was used to fit the equation.

$$Q = \sum_{i=1}^n [z_i - f(x_i, y_i)]^2 \quad (6)$$

In practical scenarios, the MHR of drivers is influenced by both driving speed and environmental features. Hence, we employed a trend surface analysis approach utilizing mathematical computations and polynomial regression fitting equations to investigate the combined impact of driving speed and road visual landscape complexity. This analysis measured the correlation between these factors and the occurrence of driver fatigue while uncovering their changing trends. The measured data included heart rate values (denoted as  $z$ ), driving speeds (denoted as  $x$ ), and landscape complexity values (denoted as  $y$ , calculated as described in Section 2.4).

$$z = a^0 + \sum_{i=1}^n (a^i x + b^i y)^i \quad (7)$$

By conducting an in-depth analysis of the model constructed based on these three factors, we can unveil the variability of driver heart rate and comprehensively assess the patterns of physiological changes during the driving process. This research holds significant implications for enhancing driving safety, optimizing driving environment design, and monitoring driver health, as it helps to establish the correlation between driving environment and physiological data.

To investigate the extent of driver heart rate variation with changes in road landscape complexity and driving speed, a sensitivity analysis was performed on the constructed model. Sensitivity analysis encompasses both single and multi-factor sensitivity analyses. Single-factor sensitivity analysis focuses on studying the impacts of individual parameter variations on the target, whereas multi-factor sensitivity analysis considers the combined effects of various parameter combinations on the target. The distinction between single and multi-factor sensitivity analyses lies in the consideration of the interactions between the parameters [16]. Because there is no interaction between driving speed and landscape complexity, we opted for a single-factor sensitivity analysis. Using the sensitivity coefficient Formula (8), with the driver’s heart rate as the evaluation metric and driving speed and landscape complexity as influencing factors, we explored the sensitivity of each metric to the other influencing factors under the condition of holding one influencing factor constant.

$$E = \Delta H / \Delta F \tag{8}$$

In this equation, E represents the sensitivity coefficient, ΔF represents the change rate of the influencing factor F, and ΔH represents the corresponding change rate of the target when the influencing factor varies.

### 3. Results

After analyzing the 990 BSVIs used in the case study, the coverage rate of 24 frequently occurring object categories was close to 92%. These categories can be considered fundamental visual elements that constitute the driver’s highway environmental landscape. The classification and proportions of visual elements are shown in Figures 6 and 7. Within static and dynamic elements, there are both natural features and man-made structures. Sky, roads, buildings, and vegetation are the most common elements encountered by drivers while driving on a circumferential highway.

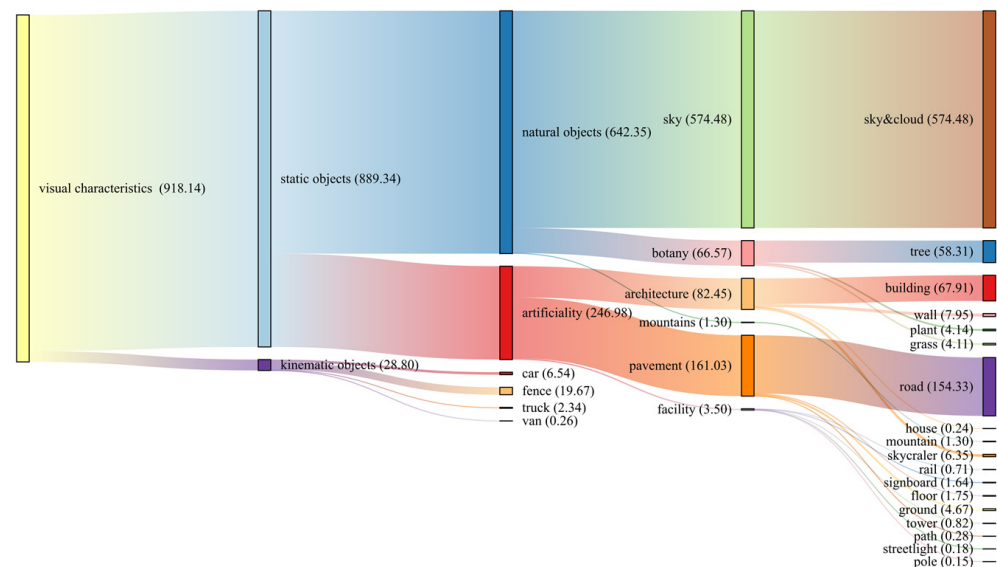
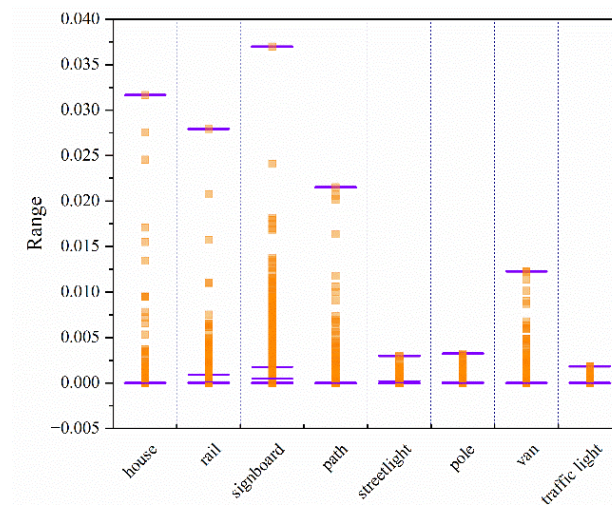
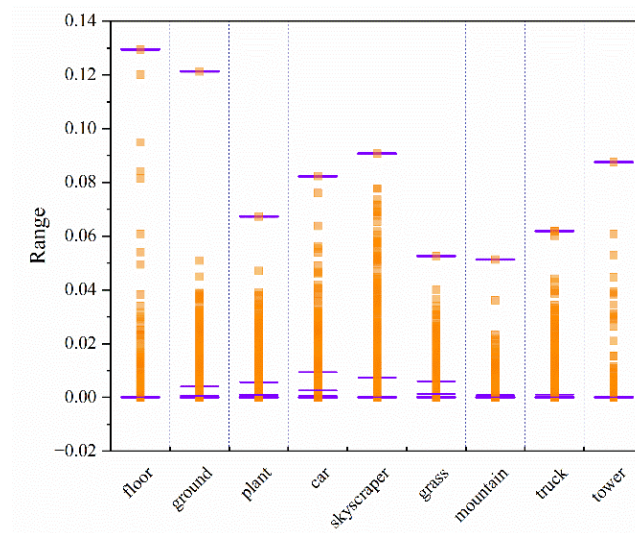


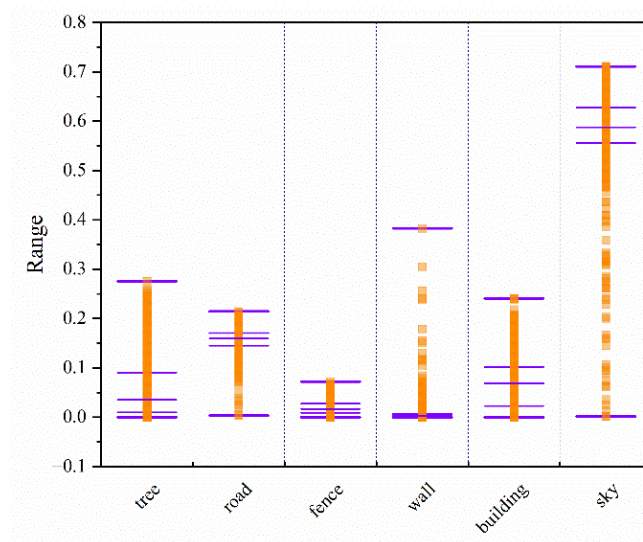
**Figure 6.** Proportional distribution of visual features of the road environment. Note: The numbers in the chart are in permille (‰) units.



(a) Low percentage visual landscape elements



(b) Moderate percentage visual landscape elements



(c) High percentage visual landscape elements

**Figure 7.** Distribution of visual landscape elements in Baidu Street View Images as a percentage of the score area.

### 3.1. Spatial Distribution Characteristics of Urban Street Visual Landscape Elements

#### 3.1.1. Spatial Distribution of Different Visual Landscape Elements

The main visual landscape elements of the urban road environment are the green-looking ratio, street openness (sky view ratio), building view index, and landscape complexity. According to the descriptive statistical analysis, the average values of the green-looking ratio, street openness, building view index, and landscape complexity were 0.067, 0.580, 0.080, and 0.351, respectively (Table 2). This indicates that the overall greenery level in the urban areas traversed by the highway was relatively low, with high openness, building density and moderate landscape complexity. The green-looking ratio, street openness, building view index, and landscape complexity varied significantly at different locations, indicating spatial heterogeneity and richness of visual landscape elements in the area (Figure 8).

**Table 2.** Basic information of visual landscape elements ( $n = 990$ ).

	Mean	Max	Min	STDEV
Green-looking ratio	0.067241	0.276717	0.000063	0.064517
Street openness	0.579668	0.710748	0.001417	0.095404
Building view index	0.075982	0.248327	0.000003	0.054918
Complexity	0.351175181	8.3073563501	0.8013822653	0.436496803

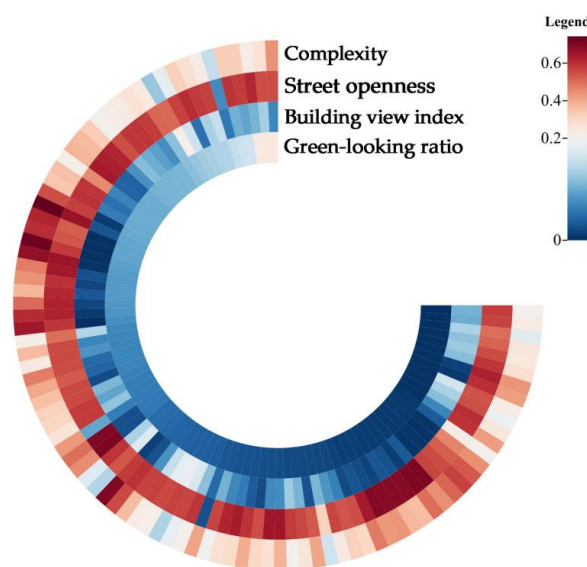


**Figure 8.** Heat map of green-looking ratio, street openness, building view index, and landscape complexity.

The areas along the peripheral expressway generally exhibited a lower green-looking ratio, with a spatial distribution showing an “east high, west low” pattern (Figure 9a). There was a significant spatial heterogeneity in the green-looking ratio within the region, indicating substantial differences in the green perceptions of drivers passing through this area. Regions with a higher building view index tended to have lower green-looking ratios, possibly because of the limited green spaces as a result of high-density architectural clusters.

The spatial distribution of street openness showed an increasing trend with increasing distance from the city center (Figure 9b). Higher street openness values were primarily concentrated along the Chan River and Yanming Lake areas, which are typically linear waterfront areas and leisure parks with lower building density and wider visibility [67,68]. Notably, despite the relatively high green-looking ratio in the Qujiang Cultural Tourism and Residential Integration Zone, street openness was relatively low [69]. Previous studies have suggested that complex street trees can affect sky openness and decrease street openness, which is consistent with the findings of this study [22]. These findings highlight the

influence of greenery on street openness and provide guidance for balancing greenery and visual openness in the planning of peripheral expressways. These findings highlight the influence of greenery on street openness and provide guidance for balancing greening and visual openness in the planning of the peripheral expressway.

Higher building view index values were concentrated in the central and western parts of the Yanta District (Figure 9c), such as Taibai South Road, Electronics South Street, Zhuque Avenue South Section, Chang'an South Road, Cuihua Road, and Yanta South Road. These areas are mainly high-tech industrial development zones, financial centers, business districts, historical and cultural quarters, and residential communities. High-density architectural clusters increase the proportion of buildings from a human perspective and create a sense of enclosure. In contrast, the eastern section of the road passes through a large heritage protection area characterized by a sparser urban structure and more open spaces, such as scenic spots, squares, parks, and rivers [70]. Consequently, the building view index remains at a lower level in this region.

Figure 9d shows the distribution trend of landscape complexity, with lower values in the western region and higher values in the eastern region. This trend was generally opposite to the distribution trend for green-looking ratio but exhibits similar heterogeneity characteristics as street openness and building view index. This distribution pattern was influenced by factors such as billboards, signboards, and construction barriers, as observed in the analysis of street-view images. Additionally, the natural environment and population density influenced landscape complexity. Areas closer to urban rivers and lakes had higher landscape complexity [71], while areas near dense residential zones tended to have stable landscape complexities.

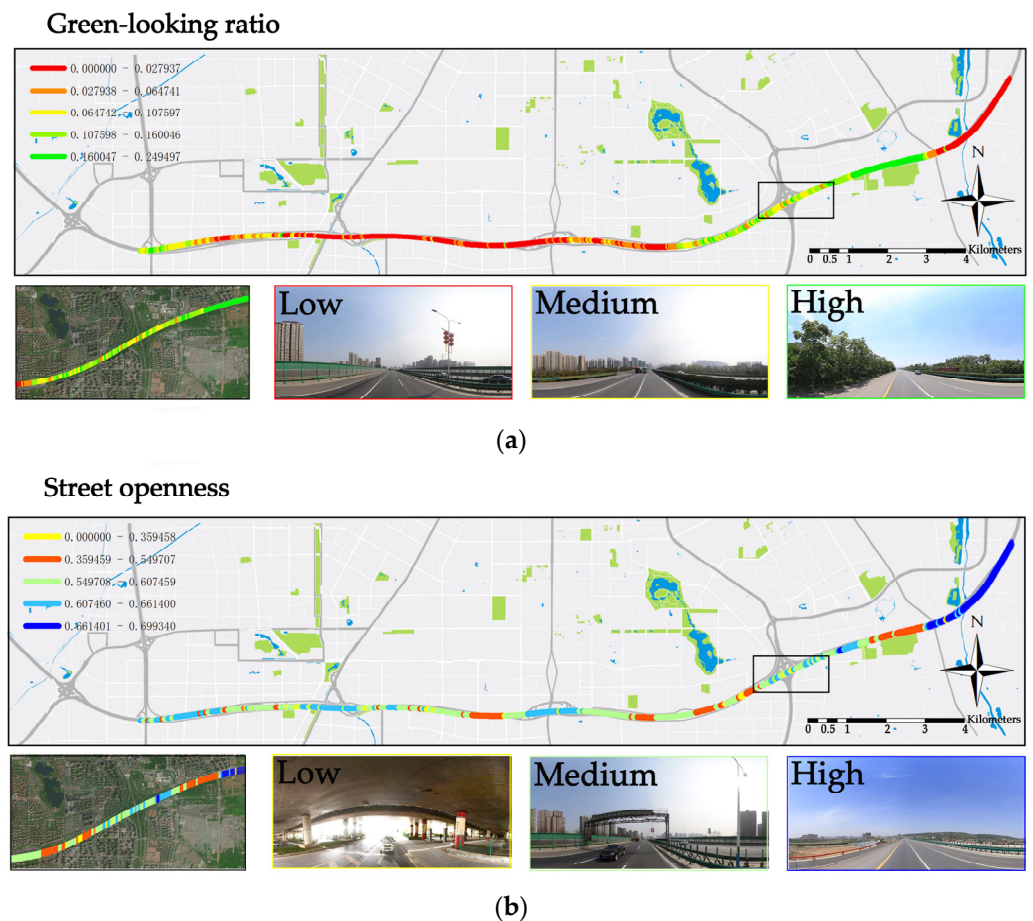
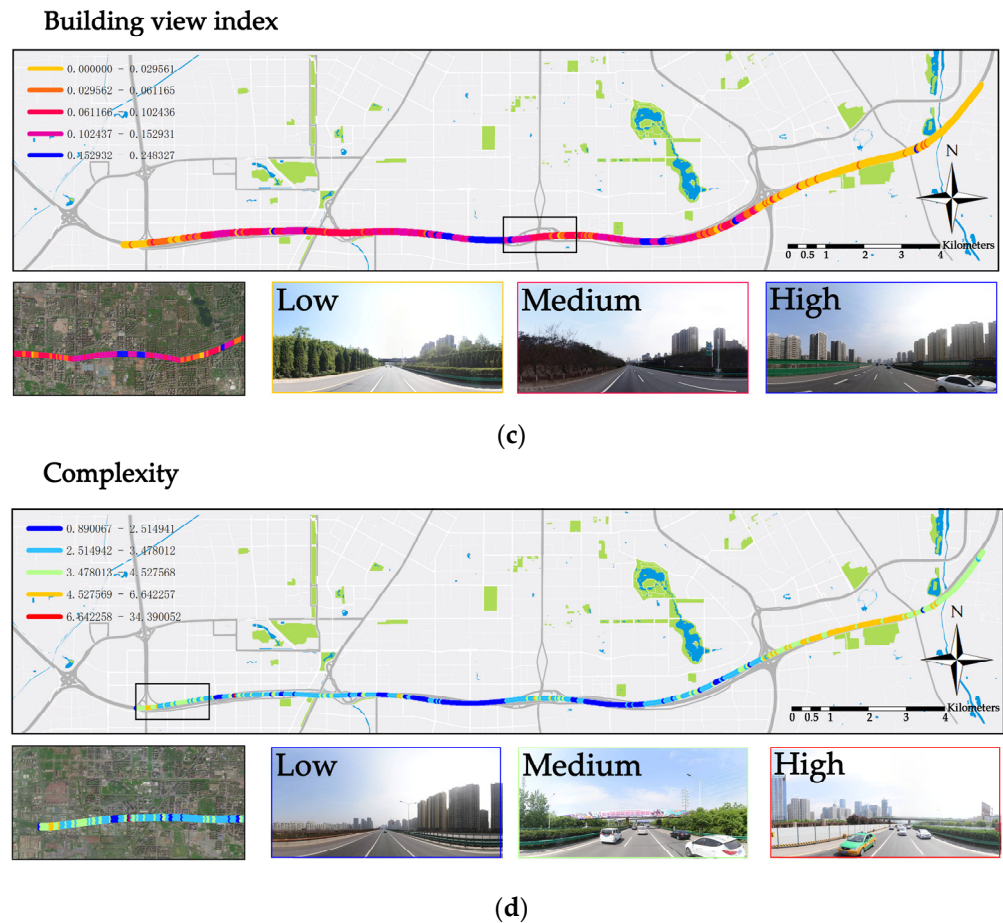


Figure 9. Cont.



**Figure 9.** Spatial distribution of visual landscape elements. (a) Distribution of green-looking ratio; (b) Distribution of street openness; (c) Distribution of building view index; (d) Distribution of complexity.

### 3.1.2. Cluster Analysis and Spatial Distribution of Visual Landscape Elements

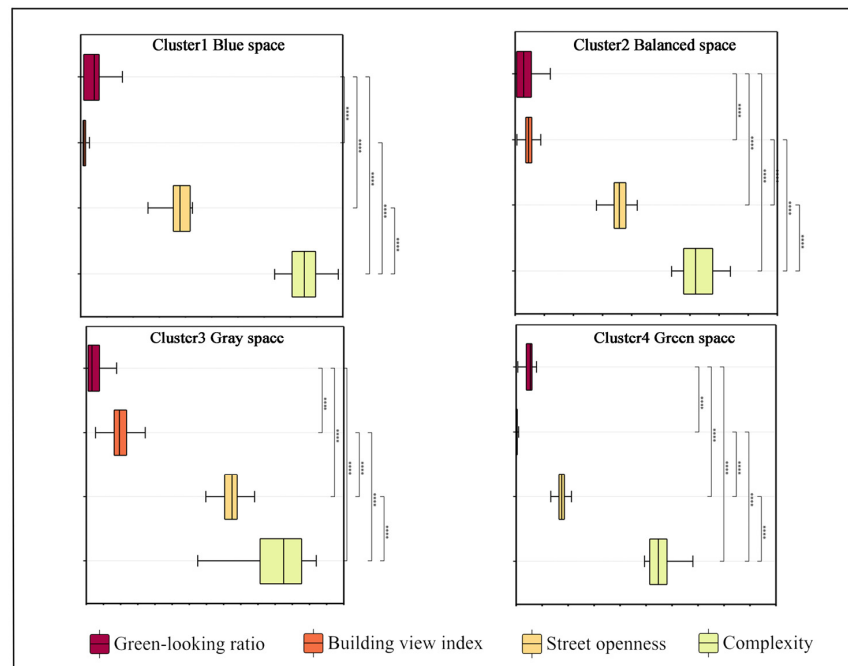
To investigate the spatial distribution patterns of the visual landscape elements along the ring road, a K-means cluster analysis was conducted on the green-looking ratio, street openness, building view index, and landscape complexity. According to the Elbow method [72], the appropriate number of clusters was determined to be 4. The analysis yielded four clusters representing areas dominated by high-complexity green spaces, low-complexity grey spaces dominated by buildings, medium-complexity blue spaces dominated by the sky, and balanced spaces with relatively even distributions of the three elements (Figure 10). The cluster centroids were as follows: 0.166, 0.009, 0.574, and 5.562 for green-dominated high-complexity spaces; 0.032, 0.135, 0.541, and 2.231 for building-dominated low-complexity spaces; 0.081, 0.027, 0.620, and 4.263 for sky-dominated medium-complexity spaces; and 0.057, 0.078, 0.589, and 3.134 for balanced spaces.



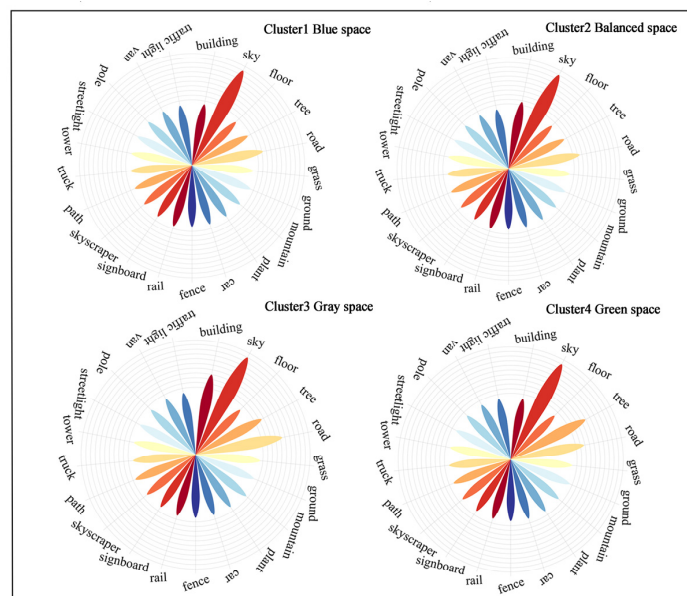
**Figure 10.** Cont.



(b)



(c)



(d)

**Figure 10.** Cluster analysis results. (a) Cluster distribution results; (b) Examples of clustered street view images; (c) Box diagrams of 4 clusters; (d) Rose charts of 4 clusters. Notes: \*\*\*\* in (c) indicates a significant difference in the levels of visual landscape element indicators within the group.

### 3.2. Impact of Visual Landscape on Driving Fatigue

#### 3.2.1. Model Fitting and Model Validation

There are two types of fatigue: active and passive [73]. Active fatigue arises from factors such as a lack of subjective engagement, monotonous external environments, or a dearth of stimulation. Prolonged or intense stress responses are the root causes of active fatigue. Under active fatigue, sympathetic nervous system tension increases, leading to an increase in MHR. Driving fatigue falls under the category of active fatigue because it is triggered by driving demands. According to the experimental data from the 31 driver groups (Figure 11), when the vehicle was traveling at speeds of 60–64 km/h, the road landscape complexity was concentrated between 1.000 and 2.000. During this stage, the overall values of the average heart rate were relatively high and stable, indicating that the barren and unchanging landscape did not have a significant positive effect on alleviating driver fatigue. However, when the driving speed was in the range of 65–83 km/h, the landscape elements became more varied, and the complexity distribution ranged from 1.298 to 8.307. The MHR values fluctuated between 91.760 and 98.560, suggesting that as the road landscape gradually became richer and more visible, the average heart rate values underwent significant changes and showed a sustained decrease in overall levels. This indicates that road landscape complexity has a positive effect on alleviating driver fatigue. Overall, as the driving speed increased and the landscape complexity fluctuated, fatigue was alleviated, leading to a downward trend in the driver's MHR.

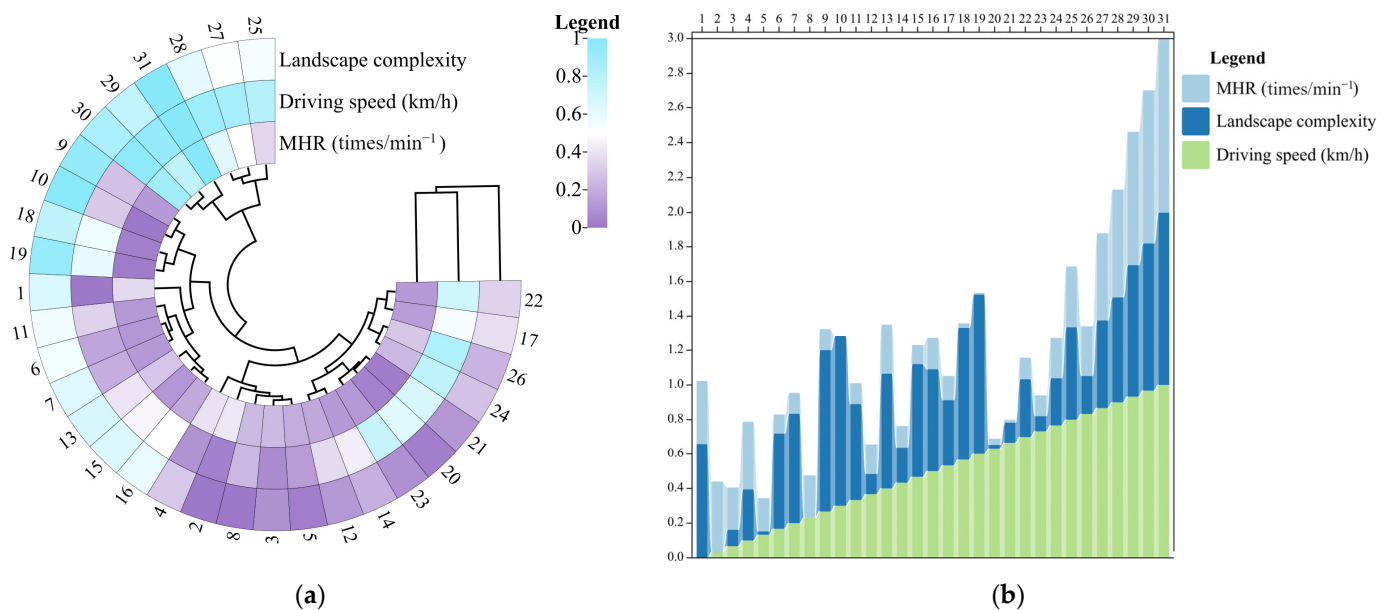


**Figure 11.** Experimental data. (a) Heat map of experimental data; (b) Histogram of experimental data.

Ridge regression analysis of the 31 datasets revealed that the variance inflation factor values were  $<10$ , indicating the absence of multicollinearity among the independent variables. The data trends also conformed to trend surface fitting using the least-squares method. By applying regression analysis to the processed data, the following non-linear regression equation was obtained:  $z = f(x, y)$ , where  $x$  represents driving speed (km/h),  $y$  represents landscape complexity, and  $z$  represents heart rate (beats/min). The coefficient for  $x^2$  was 0.859; for  $y^2$ , it was  $-0.582$ ; for  $xy$ , it was  $-0.613$ ; for  $x$ , it was  $-1.270$ ; and for  $y$ , it was 0.348. The constant term was 0.844.

Correlation tests were conducted to assess the goodness of fit and evaluate the fitting performance of the model. The root mean square error (RMSE) of the fitting model was 0.16, indicating a small error. The coefficient of determination ( $R^2$ ) was 0.465, indicating a large determination coefficient and good regression effect. This confirmed that the fitting equation could be applied to the model. The model achieved the purpose of analyzing

driving activities to some extent. From the analysis, it can be inferred that, in general, both independent variables had a positive effect on alleviating driving fatigue. As the driving speed and landscape complexity increased, the MHR tended to decrease in an overall downward trend, with the magnitude of change increasing. Driving speed had a greater impact on MHR than landscape complexity. The constructed model effectively expressed the combined influence of landscape complexity and driving speed on MHR in the peripheral visual environment of the expressway.

### 3.2.2. Sensitivity Analysis

As shown in Figure 12, several scenarios were tested to examine the rate of change in heart rate values with variations in landscape complexity and driving speed at fixed increments of 100%. This allowed us to determine the sensitivity coefficients of the heart rate values to the influencing factors. The increment in heart rate was relatively larger with changes in driving speed, indicating a greater sensitivity of heart rate to driving speed. This suggests that heart rate values can effectively reflect driver fatigue. Landscape complexity was found to be closely related to fluctuations in heart rate values. Driver fatigue induced by landscapes is classified as active fatigue. With an increase in the magnitude of landscape complexity fluctuations, the amplitude of heart rate value fluctuations also increased to some extent, indicating that drivers are less prone to fatigue in such situations. Overall, by comparing  $E(\text{MHR}, \text{complexity})$  and  $E(\text{MHR}, \text{driving speed})$ ,  $E(\text{MHR}, \text{complexity})$  was smaller than  $E(\text{MHR}, \text{driving speed})$ , indicating that heart rate values were more sensitive to driving speed than landscape complexity. The effect of driving speed on driver fatigue was greater than that of landscape complexity.

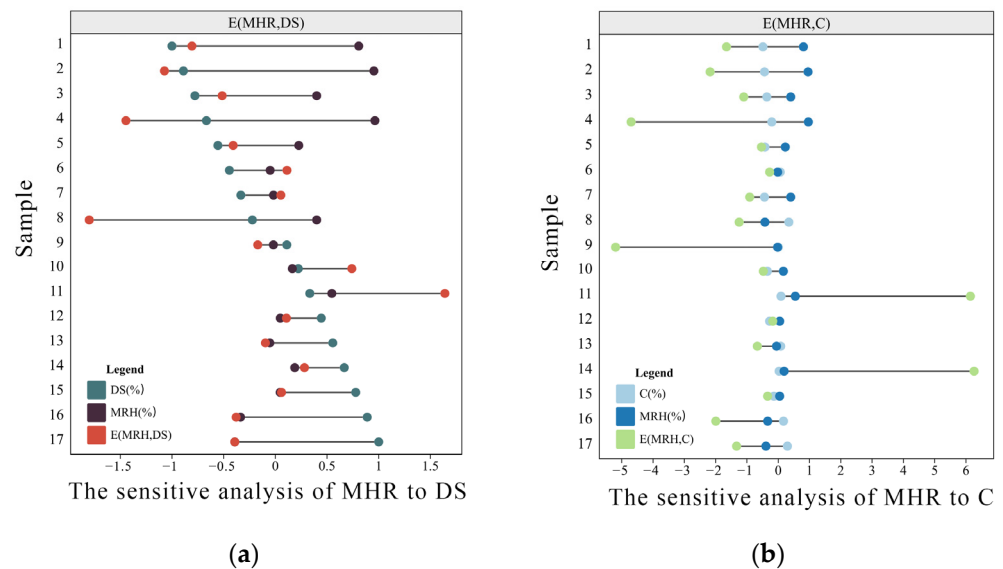


**Figure 12.** Sensitive analysis. (a)  $E(\text{MHR}, \text{DS})$ ; (b)  $E(\text{MHR}, \text{C})$ . Abbreviations: E, sensitivity coefficient; MHR, mean heart rate; DS, driving speed; C, complexity.

## 4. Discussion

Driving is a demanding task, and road landscapes heavily consume driver attention through visual perception [74,75]. In highly urbanized areas, landscapes with little to no visual elements require drivers to exert significant directional attention, leading to adverse driving reactions [76]. Driving performance decreases when attention fatigue sets in [77]. Therefore, the impact of the environment on drivers is crucial because prolonged exposure to monotonous environments can result in visual fatigue, ultimately affecting driving safety. Well-designed road landscapes help alleviate adverse reactions caused by long-duration driving. Visual contact with landscapes helps restore attention and mitigate driving fatigue. Consequently, landscapes can improve driving performance by alleviating driver fatigue.

Previous studies have shown that using large-scale street-image datasets and deep-learning algorithms can expand the extent of our understanding of the influence of landscape attributes on perception [78,79]. Using computer vision techniques, various pieces of information can be extracted from street-view images, such as road morphology, road feature composition, and road greening [80]. The detection of red, green, and blue bands from street-view images and the calculation of the differences between these bands can assess the greening status at the street level and determine the area of green vegetation [81]. Other studies have utilized photographic methods to quantify several visual factors of street canyons, such as the sky, trees, and buildings.

However, previous research often lacked sufficient data, with street-image sampling locations primarily limited to specific communities or captured manually using cameras. However, such surveys are costly, time-consuming, and have limited sample sizes. Most studies investigating the influence of urban physical environments on individuals rely on participant ratings [82] or geographical information system-derived measures [83], with limited literature on perceptions and behaviors observed after viewing visual road environments. Given the significant differences in regulations and speeds between highways and local roads and streets [84], most research on the impact of landscapes on highway driving has focused on driver-vehicle dynamics and kinematic principles, with studies involving human visual perception concentrating on eye movement observations [85,86]. Therefore, research that combines multiple visual landscape elements and interprets their relationships with driver perception, which is linked to traffic safety, is unique when conducted on peripheral expressways.

Based on the developed FCN model, this study proposes a framework for effectively extracting road visual elements from street view images. Referring to 151 elements from previous research as input, the model is trained for image segmentation with proportions. Furthermore, specific landscape and visual elements, including buildings, roads, trees, grass, and the sky, are found to have the highest weights, indicating their significant impact on drivers' states. Utilizing 31 sets of data from real vehicle experiments, a quantitative model is established to study the influence of road visual landscape on driving fatigue. Sensitivity analysis is conducted, validating that urban traffic landscape elements can affect driving fatigue and, consequently, road safety. The influence of buildings and the sky on visual surroundings, as well as the fatigue-reducing effect of greenery, are confirmed. These findings can contribute to improving the driving experience in practice and provide new perspectives for urban planning and road design with a focus on road traffic safety.

This study had several limitations. The research utilized the semantic segmentation results of road landscape cross-sections as variables for the fitting model, with limited consideration of urban landscape changes along the road's longitudinal section. Future work could explore longitudinal landscape variations and examine the influence of spatial autocorrelation of surrounding parks, communities, and campuses. Street-view images are not frequently updated; thus, they fail to capture changes related to time, weather, and other factors [87], whereas human states can be influenced by factors beyond visual stimuli. This research attempted to overcome the limitations of fixed time and single perspectives in street-view images by incorporating different groups representing seasonal changes, weather conditions, and other relevant factors to enhance the realism of the investigation.

## 5. Conclusions

Road landscapes provide a variety of visual experiences, and quantifying their perceptual characteristics has always been a challenge. This study utilizes deep learning techniques to interpret street-view images, achieve quantification and spatial distribution analysis of visual perception in road environments, and make initial efforts to understand the impact of road landscapes on driver psychological states. The study revealed the following conclusions. First, the spatial distribution characteristics of road visual landscapes exhibited a pattern of aggregation according to urban functional features. Overall, the level of street openness was good, whereas the abundance of green visual elements was

relatively low, especially in residential communities closer to the city center. Second, the spatial distribution of visual landscape elements shows obvious variations, with central areas having a dense and balanced building distribution, higher complexity, and better quality of landscapes as the proximity to urban rivers and lakes increases [88]. Third, the 31 sets of data collected from the experiment demonstrate that roadside landscapes have a significant impact on driving states, primarily through the influence of landscape complexity on the driver's heart rate. When passing through areas with higher complexity, a change of approximately 10% in the landscape complexity resulted in a fluctuation of approximately 0.2% in the driver's heart rate. Specifically, when the landscape complexity ranges from 5.28 to 8.30, the heart rate showed noticeable fluctuations between 91 and 96. This change in heart rate may help drivers alleviate fatigue, reduce suppressed driving fatigue, and achieve the goal of maintaining alertness.

Road landscape is an essential component of highway infrastructure, providing a buffer for driving activities in high-density urban environments and demonstrating measurable benefits in reducing fatigue. This research contributes to the transportation field by offering valuable insights for policymakers and design professionals. It advocates a people-centric approach in planning roadside landscapes, focusing on their impact on driver health and safety. Emphasizing the expansion of green vegetation and enhancing landscape complexity effectively improves the driving environment. Road infrastructure departments can utilize the research findings to ensure a rational layout of road landscape, creating visually pleasant experiences for drivers and ultimately reducing the likelihood of traffic accidents through strengthened traffic safety management. From a driver's perspective, this study promises a safer and more comfortable driving experience. Well-planned road landscapes not only alleviate visual fatigue but also enhance driver alertness, mitigating driver fatigue and boosting driving safety. Considering the support of open-source street view imagery data, this study's proposed methods can further quantify perceptions of different types of traffic landscape spaces. This extension enhances the application of landscapes in traffic safety, providing fresh ideas and approaches to promote driver and passenger health and safety at a macroscopic level. Overall, this research contributes to the sustainable development of the transportation field and offers valuable guidance for driver safety and well-being.

**Author Contributions:** Conceptualization, L.L. and P.L.; methodology, L.L., P.L. and Z.G.; validation, Z.G. and M.H.; formal analysis, Z.G.; data curation, Z.G.; writing—original draft preparation, L.L., Z.G. and M.R.R.M.A.Z.; writing—review and editing, L.L., P.L., M.H.Z. and W.D.; visualization, Z.G.; supervision, L.L., P.L., M.H. and W.D. All authors have read and agreed to the published version of the manuscript.

**Funding:** This research was supported by the 2023 Social Science Planning Fund Project in Xi'an City (No.: 23LW184), the Research Project on Ecological Space Governance Key Project of Shaanxi Province (No.: 2022HZ1861), the 2022 Social Science Planning Fund Project in Xi'an City (No.: 22LW156), China Scholarship Council (Grant No.: Liujinmei [2022] No. 45; Liujinxuan [2022] No. 133; Liujinou [2023] No. 22), International Education Research Program of Chang'an University (300108221102), Project of Ningxia Natural Science Foundation (2022AAC03700; 2022BEG03059), 2022 Guangdong University Youth Innovation Talent Program (2022KQNCX143) and Yinshanbeilu Grassland Eco-hydrology National Observation and Research Station, China Institute of Water Resources and Hydropower Research, Beijing 100038, China, Grant NO.YSS2022004.

**Data Availability Statement:** Not applicable.

**Acknowledgments:** The authors gratefully thank the editors and anonymous reviewers for their valuable advice in improving this manuscript.

**Conflicts of Interest:** The authors declare no conflict of interest.

## References

1. Guo, B.; Wu, H.; Pei, L.; Zhu, X.; Zhang, D.; Wang, Y.; Luo, P. Study on the spatiotemporal dynamic of ground-level ozone concentrations on multiple scales across China during the blue sky protection campaign. *Environ. Int.* **2022**, *170*, 107606. [[CrossRef](#)] [[PubMed](#)]
2. Wang, X.; Luo, P.; Zheng, Y.; Duan, W.; Wang, S.; Zhu, W.; Zhang, Y.; Nover, D. Drought Disasters in China from 1991 to 2018: Analysis of Spatiotemporal Trends and Characteristics. *Remote Sens.* **2023**, *15*, 1708. [[CrossRef](#)]
3. Naik, B.; Tung, L.-W.; Zhao, S.; Khattak, A.J. Weather impacts on single-vehicle truck crash injury severity. *J. Saf. Res.* **2016**, *58*, 57–65. [[CrossRef](#)] [[PubMed](#)]
4. Zhao, S.; Khattak, A.J. Injury severity in crashes reported in proximity of rail crossings: The role of driver inattention. *J. Transp. Saf. Secur.* **2018**, *10*, 507–524. [[CrossRef](#)]
5. Yijun, X.; Junfeng, G.; Yong, Y.; Xiaolin, Y.; Wentao, H. Classifying Driving Fatigue Based on Combined Entropy Measure Using EEG Signals. *Int. J. Control Autom.* **2016**, *9*, 329–338.
6. Parsons, R.; Tassinari, L.G.; Ulrich, R.S.; Hebl, M.R.; Grossman-Alexander, M. The View from the Road: Implications for Stress Recovery and Immunization. *J. Environ. Psychol.* **1998**, *18*, 113–140. [[CrossRef](#)]
7. Froment, J.; Domon, G. Viewer appreciation of highway landscapes: The contribution of ecologically managed embankments in Quebec, Canada. *Landsc. Urban Plan.* **2006**, *78*, 14–32. [[CrossRef](#)]
8. Wolf, K.L. Assessing Public Response to Freeway Roadsides: Urban Forestry and Context-Sensitive Solutions. *Transp. Res. Rec.* **2006**, *1984*, 102–111. [[CrossRef](#)]
9. Akbar, K.F.; Hale, W.H.G.; Headley, A.D. Assessment of scenic beauty of the roadside vegetation in northern England. *Landsc. Urban Plan.* **2003**, *63*, 139–144. [[CrossRef](#)]
10. Edquist, J.; Rudin-Brown, C.M.; Lenné, M.G. The effects of on-street parking and road environment visual complexity on travel speed and reaction time. *Accid. Anal. Prev.* **2012**, *45*, 759–765. [[CrossRef](#)]
11. Atombo, C.; Wu, C.; Zhong, M.; Zhang, H. Investigating the motivational factors influencing drivers intentions to unsafe driving behaviours: Speeding and overtaking violations. *Transp. Res. Part F Traffic Psychol. Behav.* **2016**, *43*, 104–121. [[CrossRef](#)]
12. Anciaes, P. Effects of the roadside visual environment on driver wellbeing and behaviour—A systematic review. *Transp. Rev.* **2023**, *43*, 571–598. [[CrossRef](#)]
13. Antonson, H.; Jägerbrand, A.; Ahlström, C. Experiencing moose and landscape while driving: A simulator and questionnaire study. *J. Environ. Psychol.* **2015**, *41*, 91–100. [[CrossRef](#)]
14. Marshall, P.E.W.E.; Coppola, N.; Golombek, Y. Urban clear zones, street trees, and road safety. *Res. Transp. Bus. Manag.* **2018**, *29*, 136–143. [[CrossRef](#)]
15. Lin, X.; Zhang, J.; Liu, Z.; Shen, J. Semi-automatic extraction of ribbon roads from high resolution remotely sensed imagery by T-shaped template matching. In Proceedings of the Geoinformatics 2008 and Joint Conference on GIS and Built Environment: Classification of Remote Sensing Images, Guangzhou, China, 29–29 June 2008; Volume 7147.
16. Kong, W.; Wang, T.; Liu, L.; Luo, P.; Cui, J.; Wang, L.; Hua, X.; Duan, W.; Su, F. A novel design and application of spatial data management platform for natural resources. *J. Clean. Prod.* **2023**, *411*, 137183. [[CrossRef](#)]
17. Dai, J.; Zhu, T.; Zhang, Y.; Ma, R.; Li, W. Lane-Level Road Extraction from High-Resolution Optical Satellite Images. *Remote Sens.* **2019**, *11*, 2672. [[CrossRef](#)]
18. Liu, L.; Wu, R.; Lou, Y.; Luo, P.; Sun, Y.; He, B.; Hu, M.; Herath, S. Exploring the Comprehensive Evaluation of Sustainable Development in Rural Tourism: A Perspective and Method Based on the AVC Theory. *Land* **2023**, *12*, 1473. [[CrossRef](#)]
19. Ali, F.; Ali, A.; Imran, M.; Naqvi, R.A.; Siddiqi, M.H.; Kwak, K.-S. Traffic accident detection and condition analysis based on social networking data. *Accid. Anal. Prev.* **2021**, *151*, 105973. [[CrossRef](#)]
20. Treash, K.; Amaratunga, K. Automatic Road Detection in Grayscale Aerial Images. *J. Comput. Civ. Eng.* **2000**, *14*, 60–69. [[CrossRef](#)]
21. Schubert, H.; van de Gronde, J.J.; Roerdink, J.B.T.M. Efficient Computation of Greyscale Path Openings. *Math. Morphol. Theory Appl.* **2016**, *1*, 189–202. [[CrossRef](#)]
22. Ito, K.; Biljecki, F. Assessing bikeability with street view imagery and computer vision. *Transp. Res. Part C Emerg. Technol.* **2021**, *132*, 103371. [[CrossRef](#)]
23. Larkin, A.; Gu, X.; Chen, L.; Hystad, P. Predicting perceptions of the built environment using GIS, satellite and street view image approaches. *Landsc. Urban Plan.* **2021**, *216*, 104257. [[CrossRef](#)] [[PubMed](#)]
24. Pamukcu-Albers, P.; Ugolini, F.; La Rosa, D.; Grădinaru, S.R.; Azevedo, J.C.; Wu, J. Building green infrastructure to enhance urban resilience to climate change and pandemics. *Landsc. Ecol.* **2021**, *36*, 665–673. [[CrossRef](#)] [[PubMed](#)]
25. Zuurbier, M.; van Loenhout, J.A.F.; le Grand, A.; Greven, F.; Duijm, F.; Hoek, G. Street temperature and building characteristics as determinants of indoor heat exposure. *Sci. Total Environ.* **2021**, *766*, 144376. [[CrossRef](#)]
26. Zhou, H.; He, S.; Cai, Y.; Wang, M.; Su, S. Social inequalities in neighborhood visual walkability: Using street view imagery and deep learning technologies to facilitate healthy city planning. *Sustain. Cities Soc.* **2019**, *50*, 101605. [[CrossRef](#)]
27. Balali, V.; Ashouri Rad, A.; Golparvar-Fard, M. Detection, classification, and mapping of U.S. traffic signs using google street view images for roadway inventory management. *Vis. Eng.* **2015**, *3*, 15. [[CrossRef](#)]
28. Majidifard, H.; Adu-Gyamfi, Y.; Buttlar, W.G. Deep machine learning approach to develop a new asphalt pavement condition index. *Constr. Build. Mater.* **2020**, *247*, 118513. [[CrossRef](#)]

29. Cheng, G.; Zhu, F.; Xiang, S.; Pan, C. Road Centerline Extraction via Semisupervised Segmentation and Multidirection Nonmaximum Suppression. *IEEE Geosci. Remote Sens. Lett.* **2016**, *13*, 545–549. [[CrossRef](#)]
30. Gkolias, K.; Vlahogianni, E.I. Convolutional Neural Networks for On-Street Parking Space Detection in Urban Networks. *IEEE Trans. Intell. Transp. Syst.* **2019**, *20*, 4318–4327. [[CrossRef](#)]
31. Lee, D.-H.; Chen, K.-L.; Liou, K.-H.; Liu, C.-L.; Liu, J.-L. Deep learning and control algorithms of direct perception for autonomous driving. *Appl. Intell.* **2021**, *51*, 237–247. [[CrossRef](#)]
32. Wu, Y.; Abdel-Aty, M.; Zheng, O.; Cai, Q.; Zhang, S. Automated safety diagnosis based on unmanned aerial vehicle video and deep learning algorithm. *Transp. Res. Rec.* **2020**, *2674*, 350–359. [[CrossRef](#)]
33. Xie, K.; Ozbay, K.; Yang, H.; Li, C. Mining automatically extracted vehicle trajectory data for proactive safety analytics. *Transp. Res. Part C Emerg. Technol.* **2019**, *106*, 61–72. [[CrossRef](#)]
34. Cao, Z.; Yun, J. Self-Awareness Safety of Deep Reinforcement Learning in Road Traffic Junction Driving. *arXiv* **2022**, arXiv:2201.08116.
35. Tanprasert, T.; Siripanpornchana, C.; Surasvadi, N.; Thajchayapong, S. Recognizing traffic black spots from street view images using environment-aware image processing and neural network. *IEEE Access* **2020**, *8*, 121469–121478. [[CrossRef](#)]
36. Mooney, S.J.; DiMaggio, C.J.; Lovasi, G.S.; Neckerman, K.M.; Bader, M.D.; Teitler, J.O.; Sheehan, D.M.; Jack, D.W.; Rundle, A.G. Use of Google Street View to assess environmental contributions to pedestrian injury. *Am. J. Public Health* **2016**, *106*, 462–469. [[CrossRef](#)] [[PubMed](#)]
37. Li, X.; Cai, B.Y.; Qiu, W.; Zhao, J.; Ratti, C. A novel method for predicting and mapping the occurrence of sun glare using Google Street View. *Transp. Res. Part C Emerg. Technol.* **2019**, *106*, 132–144. [[CrossRef](#)]
38. Wang, S.; Zhang, K.; Chao, L.; Chen, G.; Xia, Y.; Zhang, C. Investigating the Feasibility of Using Satellite Rainfall for the Integrated Prediction of Flood and Landslide Hazards over Shaanxi Province in Northwest China. *Remote Sens.* **2023**, *15*, 2457. [[CrossRef](#)]
39. Luo, P.; Luo, M.; Li, F.; Qi, X.; Huo, A.; Wang, Z.; He, B.; Takara, K.; Nover, D. Urban flood numerical simulation: Research, methods and future perspectives. *Environ. Model. Softw.* **2022**, *156*, 105478. [[CrossRef](#)]
40. Luo, P.; Zheng, Y.; Wang, Y.; Zhang, S.; Yu, W.; Zhu, X.; Huo, A.; Wang, Z.; He, B.; Nover, D. Comparative Assessment of Sponge City Constructing in Public Awareness, Xi'an, China. *Sustainability* **2022**, *14*, 11653. [[CrossRef](#)]
41. Deng, H.; Pepin, N.C.; Chen, Y.; Guo, B.; Zhang, S.; Zhang, Y.; Chen, X.; Gao, L.; Meibing, L.; Ying, C. Dynamics of Diurnal Precipitation Differences and Their Spatial Variations in China. *J. Appl. Meteorol. Climatol.* **2022**, *61*, 1015–1027. [[CrossRef](#)]
42. Liu, L.; Chen, M.; Luo, P.; Duan, W.; Hu, M. Quantitative Model Construction for Sustainable Security Patterns in Social—Ecological Links Using Remote Sensing and Machine Learning. *Remote Sens.* **2023**, *15*, 3837. [[CrossRef](#)]
43. Wang, S.; Luo, P.; Xu, C.; Zhu, W.; Cao, Z.; Ly, S. Reconstruction of Historical Land Use and Urban Flood Simulation in Xi'an, Shannxi, China. *Remote Sens.* **2022**, *14*, 6067. [[CrossRef](#)]
44. Duan, W.; Zou, S.; Christidis, N.; Schaller, N.; Chen, Y.; Sahu, N.; Li, Z.; Fang, G.; Zhou, B. Changes in temporal inequality of precipitation extremes over China due to anthropogenic forcings. *npj Clim. Atmos. Sci.* **2022**, *5*, 33. [[CrossRef](#)]
45. Qin, J.; Duan, W.; Chen, Y.; Dukhovny, V.A.; Sorokin, D.; Li, Y.; Wang, X. Comprehensive evaluation and sustainable development of water–energy–food–ecology systems in Central Asia. *Renew. Sustain. Energy Rev.* **2022**, *157*, 112061. [[CrossRef](#)]
46. Hu, Y.; Duan, W.; Chen, Y.; Zou, S.; Kayumba, P.M.; Qin, J. Exploring the changes and driving forces of water footprint in Central Asia: A global trade assessment. *J. Clean. Prod.* **2022**, *375*, 134062. [[CrossRef](#)]
47. Li, Q.; Fan, H.; Luan, X.; Yang, B.; Liu, L. Polygon-based approach for extracting multilane roads from OpenStreetMap urban road networks. *Int. J. Geogr. Inf. Sci.* **2014**, *28*, 2200–2219. [[CrossRef](#)]
48. Xia, Y.; Yabuki, N.; Fukuda, T. Development of a system for assessing the quality of urban street-level greenery using street view images and deep learning. *Urban For. Urban Green.* **2021**, *59*, 126995. [[CrossRef](#)]
49. Chua, E.C.-P.; Tan, W.-Q.; Yeo, S.-C.; Lau, P.; Lee, I.; Mien, I.H.; Puvanendran, K.; Gooley, J.J. Heart rate variability can be used to estimate sleepiness-related decrements in psychomotor vigilance during total sleep deprivation. *Sleep* **2012**, *35*, 325–334. [[CrossRef](#)]
50. Mehler, B.; Reimer, B.; Wang, Y. *A Comparison of Heart Rate and Heart Rate Variability Indices in Distinguishing Single-Task Driving and Driving under Secondary Cognitive Workload*, Driving Assessment Conference; University of Iowa: Iowa City, IA, USA, 2011.
51. Patel, M.; Lal, S.K.; Kavanagh, D.; Rossiter, P. Applying neural network analysis on heart rate variability data to assess driver fatigue. *Expert Syst. Appl.* **2011**, *38*, 7235–7242. [[CrossRef](#)]
52. Campbell, A.; Both, A.; Sun, Q.C. Detecting and mapping traffic signs from Google Street View images using deep learning and GIS. *Comput. Environ. Urban Syst.* **2019**, *77*, 101350. [[CrossRef](#)]
53. Rzotkiewicz, A.; Pearson, A.L.; Dougherty, B.V.; Shortridge, A.; Wilson, N. Systematic review of the use of Google Street View in health research: Major themes, strengths, weaknesses and possibilities for future research. *Health Place* **2018**, *52*, 240–246. [[CrossRef](#)] [[PubMed](#)]
54. Cai, Q.; Abdel-Aty, M.; Zheng, O.; Wu, Y. Applying machine learning and google street view to explore effects of drivers' visual environment on traffic safety. *Transp. Res. Part C Emerg. Technol.* **2022**, *135*, 103541. [[CrossRef](#)]
55. Zhang, F.; Zhang, D.; Liu, Y.; Lin, H. Representing place locales using scene elements. *Comput. Environ. Urban Syst.* **2018**, *71*, 153–164. [[CrossRef](#)]
56. Bosch, M.V.D.; Sang, A.O. Urban natural environments as nature-based solutions for improved public health—A systematic review of reviews. *Environ. Res.* **2017**, *158*, 373–384. [[CrossRef](#)]

57. Guan, F.; Fang, Z.; Wang, L.; Zhang, X.; Zhong, H.; Huang, H. Modelling people's perceived scene complexity of real-world environments using street-view panoramas and open geodata. *ISPRS J. Photogramm. Remote Sens.* **2022**, *186*, 315–331. [[CrossRef](#)]
58. Calvi, A. Does Roadside Vegetation Affect Driving Performance?: Driving Simulator Study on the Effects of Trees on Drivers' Speed and Lateral Position. *Transp. Res. Rec.* **2015**, *2518*, 1–8. [[CrossRef](#)]
59. Fitzpatrick, C.D.; Samuel, S.; Knodler, M.A. Evaluating the effect of vegetation and clear zone width on driver behavior using a driving simulator. *Transp. Res. Part F Traffic Psychol. Behav.* **2016**, *42*, 80–89. [[CrossRef](#)]
60. Antonson, H.; Mårdh, S.; Wiklund, M.; Blomqvist, G. Effect of surrounding landscape on driving behaviour: A driving simulator study. *J. Environ. Psychol.* **2009**, *29*, 493–502. [[CrossRef](#)]
61. Yi, Y.K.; Kim, H. Universal Visible Sky Factor: A method for calculating the three-dimensional visible sky ratio. *Build. Environ.* **2017**, *123*, 390–403. [[CrossRef](#)]
62. Dumbaugh, E.; Saha, D.; Merlin, L. Toward Safe Systems: Traffic Safety, Cognition, and the Built Environment. *J. Plan. Educ. Res.* **2020**, *5*, 0739456X20931915. [[CrossRef](#)]
63. Theeuwes, J. Self-explaining roads: What does visual cognition tell us about designing safer roads? *Cogn. Res. Princ. Implic.* **2021**, *6*, 15. [[CrossRef](#)] [[PubMed](#)]
64. Charlton, S.G.; Mackie, H.W.; Baas, P.H.; Hay, K.; Menezes, M.; Dixon, C. Using endemic road features to create self-explaining roads and reduce vehicle speeds. *Accid. Anal. Prev.* **2010**, *42*, 1989–1998. [[CrossRef](#)] [[PubMed](#)]
65. Jiang, B.; He, J.; Chen, J.; Larsen, L.; Wang, H. Perceived Green at Speed: A Simulated Driving Experiment Raises New Questions for Attention Restoration Theory and Stress Reduction Theory. *Environ. Behav.* **2021**, *53*, 296–335. [[CrossRef](#)]
66. Frumkin, H. Urban Sprawl and Public Health. *Public Health Rep.* **2002**, *117*, 201–217. [[CrossRef](#)]
67. Wang, Z.; Luo, P.; Zha, X.; Xu, C.; Kang, S.; Zhou, M.; Nover, D.; Wang, Y. Overview assessment of risk evaluation and treatment technologies for heavy metal pollution of water and soil. *J. Clean. Prod.* **2022**, *379*, 134043. [[CrossRef](#)]
68. Chen, X.; Zhang, K.; Luo, Y.; Zhang, Q.; Zhou, J.; Fan, Y.; Huang, P.; Yao, C.; Chao, L.; Bao, H. A distributed hydrological model for semi-humid watersheds with a thick unsaturated zone under strong anthropogenic impacts: A case study in Haihe River Basin. *J. Hydrol.* **2023**, *623*, 129765. [[CrossRef](#)]
69. Lin, L.; Wei, X.; Luo, P.; Wang, S.; Kong, D.; Yang, J. Ecological Security Patterns at Different Spatial Scales on the Loess Plateau. *Remote Sens.* **2023**, *15*, 1011. [[CrossRef](#)]
70. Chen, G.; Zhang, K.; Wang, S.; Xia, Y.; Chao, L. iHydroSlide3D v1. 0: An advanced hydrological–geotechnical model for hydrological simulation and three-dimensional landslide prediction. *Geosci. Model Dev.* **2023**, *16*, 2915–2937. [[CrossRef](#)]
71. Cao, Z.; Zhu, W.; Luo, P.; Wang, S.; Tang, Z.; Zhang, Y.; Guo, B. Spatially Non-Stationary Relationships between Changing Environment and Water Yield Services in Watersheds of China's Climate Transition Zones. *Remote Sens.* **2022**, *14*, 5078. [[CrossRef](#)]
72. Ou, J.; Yang, S.; Wu, Y.J.; An, C.; Xia, J. Systematic clustering method to identify and characterise spatiotemporal congestion on freeway corridors. *IET Intell. Transp. Syst.* **2018**, *12*, 826–837. [[CrossRef](#)]
73. Desmond, P.A.; Hancock, P.A. Active and passive fatigue states. In *Stress, Workload, and Fatigue*; CRC Press: Boca Raton, FL, USA, 2000; pp. 455–465.
74. Kaplan, S. The restorative benefits of nature: Toward an integrative framework. *J. Environ. Psychol.* **1995**, *15*, 169–182. [[CrossRef](#)]
75. Sullivan, W. Fostering reasonableness: Supportive environments for bringing out our best. In *Search of a Clear Head*; Michigan Publishing: Ann Arbor, MI, USA, 2015; pp. 54–69.
76. Roe, J.; Aspinall, P. The restorative outcomes of forest school and conventional school in young people with good and poor behaviour. *Urban For. Urban Green.* **2011**, *10*, 205–212. [[CrossRef](#)]
77. Oron-Gilad, T.; Ronen, A. Road characteristics and driver fatigue: A simulator study. *Traffic Inj. Prev.* **2007**, *8*, 281–289. [[CrossRef](#)] [[PubMed](#)]
78. Rossetti, T.; Lobel, H.; Rocco, V.; Hurtubia, R. Explaining subjective perceptions of public spaces as a function of the built environment: A massive data approach. *Landsc. Urban Plan.* **2019**, *181*, 169–178. [[CrossRef](#)]
79. Ramírez, T.; Hurtubia, R.; Lobel, H.; Rossetti, T. Measuring heterogeneous perception of urban space with massive data and machine learning: An application to safety. *Landsc. Urban Plan.* **2021**, *208*, 104002. [[CrossRef](#)]
80. Middel, A.; Lukasczyk, J.; Zakrzewski, S.; Arnold, M.; Maciejewski, R. Urban form and composition of street canyons: A human-centric big data and deep learning approach. *Landsc. Urban Plan.* **2019**, *183*, 122–132. [[CrossRef](#)]
81. Li, X.; Zhang, C.; Li, W.; Ricard, R.; Meng, Q.; Zhang, W. Assessing street-level urban greenery using Google Street View and a modified green view index. *Urban For. Urban Green.* **2015**, *14*, 675–685. [[CrossRef](#)]
82. Van den Berg, M.; Wendel-Vos, W.; van Poppel, M.; Kemper, H.; van Mechelen, W.; Maas, J. Health benefits of green spaces in the living environment: A systematic review of epidemiological studies. *Urban For. Urban Green.* **2015**, *14*, 806–816. [[CrossRef](#)]
83. Nordbø, E.C.A.; Nordh, H.; Raanaas, R.K.; Aamodt, G. GIS-derived measures of the built environment determinants of mental health and activity participation in childhood and adolescence: A systematic review. *Landsc. Urban Plan.* **2018**, *177*, 19–37. [[CrossRef](#)]
84. Farahmand, B.; Boroujerdian, A.M. Effect of road geometry on driver fatigue in monotonous environments: A simulator study. *Transp. Res. Part F Traffic Psychol. Behav.* **2018**, *58*, 640–651. [[CrossRef](#)]
85. Minaee, S.; Minaei, M.; Abdolrashidi, A. Deep-emotion: Facial expression recognition using attentional convolutional network. *Sensors* **2021**, *21*, 3046. [[CrossRef](#)] [[PubMed](#)]

86. Xiao, H.; Li, W.; Zeng, G.; Wu, Y.; Xue, J.; Zhang, J.; Li, C.; Guo, G. On-road driver emotion recognition using facial expression. *Appl. Sci.* **2022**, *12*, 807. [[CrossRef](#)]
87. Kang, Y.; Zhang, F.; Gao, S.; Lin, H.; Liu, Y. A review of urban physical environment sensing using street view imagery in public health studies. *Ann. GIS* **2020**, *26*, 261–275. [[CrossRef](#)]
88. Zhu, W.; Cao, Z.; Luo, P.; Tang, Z.; Zhang, Y.; Hu, M.; He, B. Urban Flood-Related Remote Sensing: Research Trends, Gaps and Opportunities. *Remote Sens.* **2022**, *14*, 5505. [[CrossRef](#)]

**Disclaimer/Publisher’s Note:** The statements, opinions and data contained in all publications are solely those of the individual author(s) and contributor(s) and not of MDPI and/or the editor(s). MDPI and/or the editor(s) disclaim responsibility for any injury to people or property resulting from any ideas, methods, instructions or products referred to in the content.